Journal of Photochemistry & Photobiology, B: Biology 206 (2020) 111863

Contents lists available at ScienceDirect

Journal of Photochemistry & Photobiology, B: Biology

journal homepage: www.elsevier.com/locate/jphotobiol

Farnesol potentiates photodynamic inactivation of *Staphylococcus aureus* with the use of red light-activated porphyrin TMPyP

Monika Kossakowska-Zwierucho[a,*], Grzegorz Szewczyk[b], Tadeusz Sarna[b], Joanna Nakonieczna[a,*]

[a] Laboratory of Molecular Diagnostics, Intercollegiate Faculty of Biotechnology University of Gdansk and Medical University of Gdansk, Gdansk, Poland
[b] Department of Biophysics, Faculty of Biotechnology, Jagiellonian University, Krakow, Poland

ARTICLE INFO

Keywords:
Photodynamic inactivation
Staphylococcus aureus
Membrane fluidity
Reactive oxygen species detection

ABSTRACT

Photodynamic inactivation (PDI) or antibacterial photodynamic therapy (aPDT) is a method based on the use of a photosensitizer, light of a proper wavelength and oxygen, which combined together leads to an oxidative stress and killing of target cells. PDI can be applied towards various pathogenic bacteria independently on their antibiotic resistance profile. Optimization of photodynamic treatment to eradicate the widest range of human pathogens remains challenging despite the availability of numerous photosensitizing compounds. Therefore, a search for molecules that could act as adjuvants potentiating antibacterial photoinactivation is of high scientific and clinical importance. Here we propose farnesol (FRN), a well described sesquiterpene, as a potent adjuvant of PDI, which specifically sensitizes *Staphylococcus aureus* to 5,10,15,20-tetrakis(1-methylpyridinium-4-yl)porphyrin tetratosylate (TMPyP) upon red light irradiation. Interestingly, the observed potentiation strongly depends on the presence of light. Analysis of this combined action of FRN and TMPyP, however, showed no influence of farnesol on TMPyP photochemical properties, i.e. the amount of reactive oxygen species that were produced by TMPyP in the presence of FRN. The accumulation rate of TMPyP in *Staphylococcus aureus* cells did not change, as well as the influence of staphyloxanthin inhibition. The precise mechanism of observed sensitization is unclear and probably involves specific molecular targets.

1. Introduction

One of the greatest challenges in global epidemiology is to combat pathogens that escape conventional antibiotic treatment. Among them, *Staphylococcus aureus* is known to cause a wide spectrum of diseases, from mild skin infections to life-threatening systemic disorders [1]. In contrast to the expansion of antibiotic resistance, the number of new classes of antimicrobial drugs has been limited in recent years. One of the approaches that can be used to fight multiresistant microorganisms is photodynamic inactivation (PDI). PDI utilizes the combined action of three elements: a photosensitizing compound (photosensitizer, PS), visible light at a proper wavelength and molecular oxygen. Two types of photodynamic reactions occur in the cell and result in oxidative stress; type I leads to the generation of oxygen radicals, and type II results in singlet oxygen formation. The bacteria studied thus far have not developed specific resistance to this type of oxidative stress. On the other hand, the efficacy of PDI is often heterogeneous, and the pleiotropic effect induced in bacterial cells is still not fully understood.

A variety of photosensitizers of different chemical structures and properties are available for research, including porphyrins and their cationic derivatives, phenothiazines, metal phthalocyanines and many more [2]. In recent years, several approaches have been applied to increase the efficacy and specificity of antimicrobial PDI. Apart from synthetizing new PSs of desired properties, existing compounds can be functionalized with specific antibodies [3,4] or antimicrobial peptides [5,6]. Higher effectiveness can be achieved when the photosensitizing compound is delivered via a bacteriophage [7] or encapsulated in lipid nanoparticles [8]. The use of exogenous small particles or certain compounds can also be beneficial for PDI outcome, as reported in the case of chitosan [9], silver nanoparticles [10] and antimicrobial peptides [11], as well as observed when PDI was combined with some antibiotics [12,13]. Moreover, various materials can serve as a support for PS immobilization, thus extending their possible use [14].

Farnesol (FRN), an acyclic sesquiterpene alcohol of natural origin, has different applications in various industries, including perfumery, food industry and pesticide production. Originally isolated from aromatic plants, farnesol is produced by many organisms, including humans. Farnesyl pyrophosphate is a key intermediate in the mevalonate/

* Corresponding authors at: Intercollegiate Faculty of Biotechnology University of Gdansk and Medical University of Gdansk, Laboratory of Molecular Diagnostics, Abrahama 58, 80-307 Gdansk, Poland.
E-mail address: joanna.nakonieczna@biotech.ug.edu.pl (J. Nakonieczna).

https://doi.org/10.1016/j.jphotobiol.2020.111863
Received 19 December 2019; Received in revised form 11 February 2020; Accepted 19 March 2020
Available online 21 March 2020
1011-1344/ © 2020 The Authors. Published by Elsevier B.V. This is an open access article under the CC BY-NC-ND license (http://creativecommons.org/licenses/BY-NC-ND/4.0/).

cholesterol pathway and is also used as a substrate for protein isoprenylation [15]. Due to its involvement in numerous metabolic processes, its anticancer properties have been extensively examined. Various mechanisms of action were described using HeLa S3K cells [16], MCF-7 human breast cancer cells [17] and blasts from patients with acute myeloid leukemia [18]. Farnesol is also produced by the fungus *Candida albicans* as a quorum-sensing molecule that prevents biofilm formation [19]. In this context, farnesol has been examined as an antimicrobial agent, mainly against gram-positive human pathogens. With respect to the inhibition of the growth and permeabilization of bacterial membranes, FRN has been proposed as an adjuvant in antibiotic therapy [20–22].

Here, we present the first report of using FRN to boost PDI against *S. aureus*. The specific combined action of farnesol and the cationic porphyrin - 5,10,15,20-tetrakis(1-methylpyridinium-4-yl)porphyrin tetratosylate (TMPyP) occurred upon irradiation. TMPyP is a cationic meso-substituted porphyrin, described in the literature as a potent PS with high singlet oxygen yield [23] and as a DNA intercalator and inhibitor of human telomerase with potential anticancer application [24,25]. We hypothesize that farnesol acts as an adjuvant that sensitizes *S. aureus* to red light-activated TMPyP, which is ineffective for bacterial killing when applied alone [26]. The observed phenomenon is very promising from the perspective of potential *in vivo* use, not only because both compounds have been extensively examined in eukaryotic cells but also in view of red light application, which has beneficial therapeutic uses. We examined the influence of farnesol on the photodynamic properties of TMPyP, including spectral features, reactive oxygen species generation and PS accumulation in bacteria, and evaluated selected metabolic alterations induced by FRN in *S. aureus*, which may contribute to photoinactivation outcome. The exact mechanism of this combined bactericidal action remains elusive, yet this research provides a new perspective in the search for adjuvants for antibacterial PDI.

2. Materials and Methods

2.1. Bacterial Strains, Culture Conditions and Chemicals

The *S. aureus* strains used in the study included RN6390 (a non-pigmented derivative of the 8325–4 strain containing an incomplete *rsbU* gene) [27] and SH1000 (a pigmented derivative of the 8325–4 strain containing a complete *rsbU* gene) [28]. Bacterial cultures were grown aerobically in a nutrient trypticase soy broth TSB (bioMèrieux, France) at 37 °C with shaking (150 rpm), with or without farnesol. All chemicals were purchased from Sigma-Aldrich (Germany). 1 to 10 mM stock solutions of *trans-trans*-farnesol (FRN, 96% purity) were prepared in ethanol and stored at 4 °C in the dark. 1 mM stock solutions of TMPyP (97% purity) and toluidine blue O were prepared in sterile double distilled water and stored at −20 °C in the dark. 1 mM stock solution of protoporphyrin IX (≥95%) and 20 μM stock solution of zinc phthalocyanine (97%) were prepared in DMSO and stored at −20 °C in the dark. 2 mM stock solution of 1,6-diphenyl-1,3,5-hexatriane (DPH, 98% purity) was prepared in tetrahydrofuran (Merck, Germany), and 4 μM working solution was prepared by adding 100 μl to 50 ml of 0.05 M Tris-HCl (pH 7.6). Residual tetrahydrofuran was removed from the solution by gentle flushing with nitrogen [29]. The DPH working solution was stored in the dark at 4 °C until use but for no longer than 2 weeks.

2.2. Determination of MIC and MBC

To identify the minimal inhibitory concentration (MIC) of farnesol, overnight bacterial cultures were diluted and inoculated at a concentration of 10^4 CFU/ml in 100 μl of TSB on a 96-well plate. Bacteria were grown in the presence of two-fold dilutions of FRN at 37 °C with shaking in the dark. After 24 h, the MIC was determined as the lowest concentration that caused growth inhibition (clear broth). To indicate minimal bactericidal concentration (MBC), the whole content of wells including MIC and those with higher FRN concentrations were spread onto 2% agar plates. MBC was determined as the lowest concentration resulting in the total eradication of bacteria (no colonies after 24 h). Parallel assays to determine the MIC and MBC of farnesol were conducted in the presence of a photosensitizer (20 μM). In case of MIC and MBC determination in the presence of TMPyP, the photosensitizer was added along with FRN. Experiments were performed with three independent biological experiments. In further experiments, a sub-inhibitory concentration of FRN equaled ½ MIC.

2.3. PDI

Bacterial strains were cultured for 24 h, with or without sub-inhibitory concentrations of FRN, and then diluted with fresh broth to a density of 0.4 McFarland units (10^7 CFU/ml). A total of 110 μl of each culture was loaded into a 96-well plate and incubated in the dark at 37 °C for 30 min, either with or without the addition of one of the following PSs: TMPyP, phenothiazine toluidine blue O (TBO), or protoporphyrin IX (PPIX) at 20 μM or zinc phthalocyanine (ZnPC) at 5 nM. In our experimental setup the cells were either cultured (pre-incubation) in a presence of farnesol for 24 h, and subjected to PS and light, or cells were cultured standard, and farnesol was added along with PS (co-incubation) for 30 min prior irradiation. All the necessary controls were carried out accordingly including: cells treated with PS and light, cells treated with light alone, cells cultured in the presence of farnesol for 24 h and then treated with light (no PS added), cells treated with farnesol shortly prior to light (no PS added). Before light treatments, 10 μl aliquots were collected for CFU assessment and served as dark controls. Samples were irradiated with light doses ranging from 10 to 30 J/cm^2. For the irradiation procedure, LED lamps, emitting incoherent red light (λ_{max} 632 nm) (EMD Technology, Poland), designed and produced by the Laboratory of Molecular Diagnostics, were used [30]. The technical parameters were set as follows: output power of 23.4 mW/cm^2 and energy dose of 10–30 J/cm^2. Thus, 7 min 7 s were required for every 10 J/cm^2 emitted. After irradiation with each 10 J/cm^2, 10 μl of the samples were collected to perform ten-fold serial dilutions in PBS buffer, ranging from 10^{-1} to 10^{-4}. Aliquots of each dilution were streaked onto agar plates. After overnight incubation at 37 °C, the colonies that formed were counted to assess bacterial viability. All experiments were performed with three independent biological experiments.

2.4. Accumulation of TMPyP

Bacterial strains were cultured for 24 h, with or without sub-inhibitory concentrations of FRN, and then diluted in PBS buffer to a density of 0.4 McFarland units. A total of 800 μl of bacterial suspension containing 5×10^7 CFU was centrifuged at 5000 $\times g$ for 10 min, suspended in 800 μl of fresh PBS with the addition of 20 μM TMPyP (giving 0.32 pmol per 10^3 CFU), with or without FRN. Bacteria were incubated in the dark at 37 °C for 30 min (same as in the PDI procedure) and then centrifuged. After a 1:10 dilution in PBS, the absorbance of supernatants was measured at 422 nm using a SPECORD® PLUS UV/Vis spectrophotometer (Analytik Jena, Germany). The concentration of TMPyP remaining in the supernatant after incubation with bacterial cells was calculated based on a molar extinction coefficient, $\varepsilon_{422} = 2.26 \times 10^5\ M^{-1}\ cm^{-1}$ [31]. Experiments were performed with three independent biological experiments.

2.5. Analysis of TMPyP Absorption Spectra

TMPyP (5 μM) in 1 ml of distilled water was titrated with increasing concentrations of farnesol and incubated in the dark at 37 °C for 30 min. Alternatively, samples were irradiated in a 24-well plate with red light at a dose of 20 J/cm^2. Absorption spectra were recorded using

a UV–Vis Beckman DU-640 spectrophotometer (Beckman Coulter, USA) in the range of 360–750 nm. Absorption spectra were normalized to TMPyP concentration and presented as molar absorption. Samples were prepared and measured in three independent experiments.

2.6. Analysis of TMPyP Fluorescence Spectra

TMPyP (5 μM) in 200 μl of distilled water was titrated with increasing concentrations of farnesol and incubated in the dark at 37 °C for 30 min in a 96-well black plate. Fluorescence spectra were recorded employing an EnVision® Multilabel Plate Reader (Perkin-Elmer, USA) using two excitation wavelengths in Q band and Soret region, respectively at 518 nm and 420 nm, and an emission range of 600–800 nm at 2 nm intervals. Concentration of TMPyP was 5 μM in samples excited at 518 nm and 0.05 μM in those excited at 420 nm. Samples were prepared and measured in three independent experiments.

2.7. Oxygen Species Formation

2.7.1. Time-resolved spectroscopic detection of $^1O_2$

The effect of farnesol on the photogeneration of singlet oxygen by TMPyP was analyzed by directly detecting singlet oxygen phosphorescence according to the method described elsewhere [32]. In brief, 1 ml of a phosphate-buffered (pH 7.4, 10 mM) D_2O solution of TMPyP in a 1-cm optical path quartz fluorescence cuvette (QA- 1000; Hellma, Mullheim, Germany) was excited with 440 nm light pulses generated by an integrated nanosecond DSS Nd:YAG laser system equipped with a narrow bandwidth optical parametric oscillator (NT242-1 k-SH/SFG; Ekspla, Vilnius, Lithuania). To adjust the photoexcitation energy to values appropriate for singlet oxygen phosphorescence measurements, the laser beam was attenuated with four pieces of wire mesh (light transmission of each wire mesh ~42%). An FRN solution in ethanol was added to the sample in aliquots of 3.5 μl. The near-infrared luminescence was measured perpendicularly to the excitation beam in a photon-counting mode using a thermoelectric cooled NIR PMT module (H10330–45, Hamamatsu, Japan) equipped with a 1100 nm cutoff filter and additional dichroic narrow-band filter NBP, selectable from the spectral region range of 1150–1355 nm (NDC Infrared Engineering Ltd., Bates Road, Maldon, Essex, UK). Data were collected using a computer-mounted PCI-board multichannel scaler (NanoHarp 250; PicoQuant GmbH, Berlin, Germany). Data analysis, including first-order luminescence decay fitted by the Levenberg–Marquardt algorithm, was performed by custom-written software. The acquisition time of obtaining singlet oxygen phosphorescence signals was 20 s.

2.7.2. Detection of oxygen radicals

EPR spin trapping was employed using 100 mM DMPO as a spin trap. For detection of superoxide anion samples containing TMPyP or TMPyP with the addition of 35, 70, 105 μM FRN in 90% DMSO were irradiated in EPR quartz flat cells in the resonant cavity with 402 to 508 nm (10 mW/cm^2) light derived from a 300 W high pressure compact arc xenon lamp (Cermax, PE300CE-13FM/Module300W; Perkin-Elmer Optoelectronics, GmbH, Wiesbaden, Germany) equipped with a water filter, heat-reflecting hot mirror, cutoff filter that blocked light below 390 nm and blue additive dichroic filter 505FD64–25 (Andover Corporation, Salem, NC, USA). To detect hydroxyl radicals that could be photogenerated by TMPyP in the presence of the selected concentration of farnesol, the same experimental procedure was employed as above, except distilled water was used instead DMSO. EPR samples were run using a microwave power of 10.6 mW, modulation amplitude of 0.05 mT, center field of 339.0 mT, scan width of 8 mT, and scan time of 21 s. EPR measurements were performed using a Bruker EMX-AA EPR spectrometer (Bruker BioSpin, Rheinstetten, Germany).

2.8. Carotenoid Extraction

Bacterial strains were cultured for 24 h, with or without subinhibitory concentrations of FRN, and diluted in fresh broth to OD_{600} = 2. Based on a modified protocol of Lipovsky et al. [33], five-milliliter suspensions were centrifuged at 4000 ×*g* for 10 min at 4 °C, and the cell pellets were washed with distilled water, thoroughly suspended in 1.5 ml of 99% methanol (POCH, Poland) and gently agitated for 2 h in the dark until bleached. The samples were centrifuged at 10,000 ×*g* at 4 °C for 15 min, and the absorbance of the supernatants was measured at 450 nm using a Novaspec II spectrophotometer (Pharmacia Biotech, USA). Experiments were performed with three independent biological experiments.

2.9. Bacterial Membrane Fluidity Assay

Bacteria were cultured for 24 h, with or without subinhibitory concentrations of FRN. Bacterial suspensions were prepared at a density of 4.5 McFarland units (10^8 CFU/ml) in TSB medium. Bacteria that were not cultured in the presence of FRN were incubated for 30 min with subinhibitory concentrations of FRN. Samples without FRN served as controls. Temperature-dependent membrane fluidity was quantified according to modified protocols of Bayer and Voss [29,34], as described previously [26]. Suspensions were pelleted by centrifugation (5000 ×*g*, 15 min) and then suspended in 500 μl of digestion buffer (20% [*w/v*] sucrose, 0.05 Tris-HCl [pH 7.6], 0.145 M NaCl). The bacterial cell wall was then digested with 0.8 U of lysostaphin (A&A Biotechnology, Poland) in the presence of 3 U of DNase I (EURx, Poland) for 1 h at 37 °C [29]. Protoplasts were collected by centrifugation (9000 ×*g*, 15 min) and suspended in 200 μl of fresh digestion buffer. For DPH labeling, protoplasts suspended in digestion buffer were mixed with DPH solution in a 1:1 ratio to obtain a 2 μM final concentration and incubated in the dark at 30 °C for 45 min. Spectrofluorometer FP-8500 (JASCO, USA) coupled with Spectra Manager™ software was used for fluorescence intensity and anisotropy (*r*) measurements. Analysis was carried out in a labeled cell suspension volume of 300 μl, agitated at 200 rpm, in a temperature gradient ranging from 20 to 40 °C (rate of increase, 1 °C per 1 min). A blank measurement was recorded using the unlabeled cell suspension of each strain separately, at a single initial point, as no significant changes in background fluorescence intensity of unlabeled protoplasts were observed during the whole measurement. The following parameters were used: a vertically polarized excitation wavelength of 360 nm (bandwidth 5 nm) and an emission wavelength of 426 nm (bandwidth 10 nm) analyzed through a rotating polarizer. Signals were measured for 2 s at each 2.5 °C interval. A G factor of 1.2017 was used. Experiments were performed with two to three independent biological experiments.

3. Results

3.1. Farnesol Potentiates the Bactericidal Activity of TMPyP Upon Red Light Irradiation

FRN, as an antimicrobial agent, shows bactericidal activity at certain concentration. To determine the appropriate dosage for a subinhibitory treatment, the MIC and MBC of FRN were determined. Depending on the *S. aureus* strain, the FRN MIC was in the range of 70–140 μM (Table 1). The concentrations equal to ½ MIC was used in further experiments (70 μM for SH1000 and 35 μM for RN6390). For antimicrobial PDI, we used the following four types of red light-absorbing PSs at concentrations selected in previous experiments in our laboratory [26]: TBO, PPIX, cationic meso-substituted porphyrin TMPyP and ZnPC. Strains SH1000 and RN6390, derived from the same reference strain 8325 [35], differ mainly in the status of the *rsbU* gene, which implies various phenotypic features crucial to PDI sensitivity. Therefore, both strains respond differently to PSs, such as PPIX or ZnPC

Table 1
MIC and MBC of farnesol. Concentrations were determined in three replicates in TSB broth and 20 μM TMPyP was added.

	MIC [μM]		MBC [μM]	
	FRN	FRN + TMPyP	FRN	FRN + TMPyP
SH1000	70–140	70–140	140	140
RN6390	70	70	70	70

[26]. Antibacterial PDI in the presence of FRN revealed additional interesting differences in the effectivity of the PSs (Fig. 1). Addition of FRN sensitized both strains to TBO and TMPyP, leading to a pronounced bactericidal effect of the latter PS. Maximal viability reduction in the case of TBO reached 3 $\log_{10}$ units in strain RN6390; however, in the case of TMPyP, the reduction in viable bacterial count exceeded 5 $\log_{10}$ units at the light dose of 20 J/cm^2 (values higher than 3 $\log_{10}$ units, thus 99.9% reduction, indicate a bactericidal effect [36]). Surprisingly, the bactericidal effect of ZnPC towards RN6390 (> 5 $\log_{10}$ units of viability reduction) was completely abolished in the presence of FRN. No significant change in the response of both strains to PPIX was noted. We applied two various approaches to study potentiation of PDI by FRN: in the first one cells were cultured for 24 h in the presence of FRN and then subjected to PDI, those cells were called pre-incubated. In the second approach, FRN and PS were added to standard grown cells and co-incubated for only 30 min prior to light exposure. Differences in the efficacy of PDI were observed after co-incubation of cells with PS and FRN prior to irradiation (thus when FRN was present at a final concentration in the irradiated mixture), but not when the bacteria were cultured (pre-incubated) with FRN and only then treated with PS and irradiated. The PSs examined in this study revealed various efficacies in the presence of FRN, with no characteristic pattern related to, for example, the chemical structure of the PSs, perhaps except for the fact that TBO and TMPyP are positively charged under the conditions studied. Our further analysis focused on the combination of FRN and TMPyP due to the specific potentiation of the bactericidal action. Without the addition of FRN, the photodynamic activity of red light-irradiated TMPyP was negligible under the conditions studied. Bactericidal activity was attributed to a combination of both compounds and light, since no relevant killing of *S. aureus* was observed after separate FRN and TMPyP treatment, in the dark or upon irradiation in control samples (Table 2). The combination of both compounds in the dark did not lead to bacterial killing, which was also supported by the observation that the MIC and MBC values of FRN did not depend on the presence of TMPyP (Table 1). Importantly, the observed bactericidal effect was achieved using red light, which was previously shown to be ineffective in the TMPyP-mediated photoinactivation of *S. aureus* [26].

3.2. Farnesol Does Not Affect the Spectral Properties of TMPyP

Since FRN demonstrated simultaneous action with TMPyP towards *S. aureus*, we examined whether FRN alters the spectral properties of TMPyP. Using this approach, changes in the concentration or electronic structure of TMPyP in a mixture can be inferred from the analysis of absorption spectra. TMPyP (at a concentration of 5 μM, which enabled unbiased absorbance recording) was titrated with increasing concentrations of FRN: the concentration of FRN was lower, equal and higher than that of the analyte. Samples were incubated and kept in the dark or irradiated, reflecting the conditions applied during the PDI experiment to observe the possible formation of chemical intermediates. Full-range absorption spectra of TMPyP were recorded and normalized to concentration, revealing no changes in the intensity or the position of the Sorret region and Q bands (Fig. 2A). This finding shows that the potentiation of TMPyP activity is not attributed to a change in absorance in the range covering the emission spectrum of the applied light source. In a similar experiment, we analyzed the fluorescence of TMPyP in the presence of FRN (Fig. 2B). No change in emission spectra was recorded upon incubation with increasing concentrations of FRN. The lack of alteration in TMPyP spectral properties suggests that TMPyP does not react with FRN under the applied experimental conditions and that no interaction that affects the spectral properties of TMPyP occurs.

3.3. Farnesol Does Not Affect Reactive Oxygen Species Formation by TMPyP

Without altering the structure of the PS, FRN could potentiate TMPyP photodynamic action by increasing the efficiency of the PS to generate reactive oxygen species. To verify this hypothesis, analyses of singlet oxygen and superoxide anion formation were conducted by means of time-resolved detection of $^1O_2$ phosphorescence and EPR-spin trapping of oxygen radicals, respectively (Fig. 3). As seen in the obtained results, FRN neither significantly modified the TMPyP-mediated formation and decay of singlet oxygen nor the generation of superoxide anions. In principle, farnesol could also potentiate the photodynamic efficiency of TMPyP via the formation of a cytotoxic product - a result of the farnesol interaction with singlet oxygen or/and superoxide anion. The results shown in Fig. 3 exclude this possibility. It is evident that even at the highest concentration of FRN used, the lifetime of singlet oxygen was practically unchanged, indicating a very inefficient interaction of farnesol with this reactive oxygen species. While the EPR spin trapping data may indicate a small inhibition of the formation of the DMPO-OOH spin adduct, in the presence of highest concentration of farnesol tested by us, the effect is rather inconsistent with the dramatic potentiation of the bactericidal PDI described above. Importantly, no other spin adducts developed in the presence of even the highest concentration of FRN. To test if farnesol affected possible photoformation of hydroxyl radicals, spin trapping experiments were carried out using distilled water as the solvent. Under the same experimental conditions as those employed for spin trapping of superoxide anion, only a residual signal of the DMPO-OH spin adduct was detected with little modulatory effect of farnesol (data not shown). Considering that at the very high concentration of DMPO used, most of hydroxyl radicals would have been spin-trapped the data clearly show that hydroxyl radicals are not involved in the observed potentiation of bacterial PDI by FRN. Therefore, the results indicate that the potentiation of TMPyP bactericidal action induced by FRN is not related to the modified formation and decay of reactive oxygen species photogenerated by TMPyP.

3.4. Farnesol Does Not Increase TMPyP Accumulation in S. aureus

Since the combined activity of farnesol and TMPyP cannot be attributed to the potentiation of the photodynamic properties of a PS, a possible effect on its accumulation in bacterial cells was analyzed. It has been documented in the literature that FRN can act as an adjuvant for various antibacterial agents, such as antibiotics. The major part of this synergistic action is due to the disruption of the bacterial membrane, enabling the increased penetration of the antibacterial agent [20]. To assess whether FRN facilitates the accumulation of TMPyP in bacterial cells, the uptake of a PS in aqueous solution was measured under conditions reflecting those applied during the PDI experiment. A simple spectrophotometric method was applied to directly calculate the amount of the PS that accumulated in bacterial cells or adsorbed on a cell surface, causing a decrease in TMPyP concentration in aqueous solution. The analysis, including bacteria preincubated (grown) in the presence of FRN and those coincubated with FRN and TMPyP, showed increased PS uptake in strain SH1000 after preincubation with FRN (Fig. 4). This result can be explained by a change in staphyloxanthin content, which would result in the altered composition of the bacterial membrane. However, after a short coincubation of bacteria with FRN and TMPyP, the condition with the maximal bactericidal effect, an increase in PS uptake was not observed. This finding showed that FRN

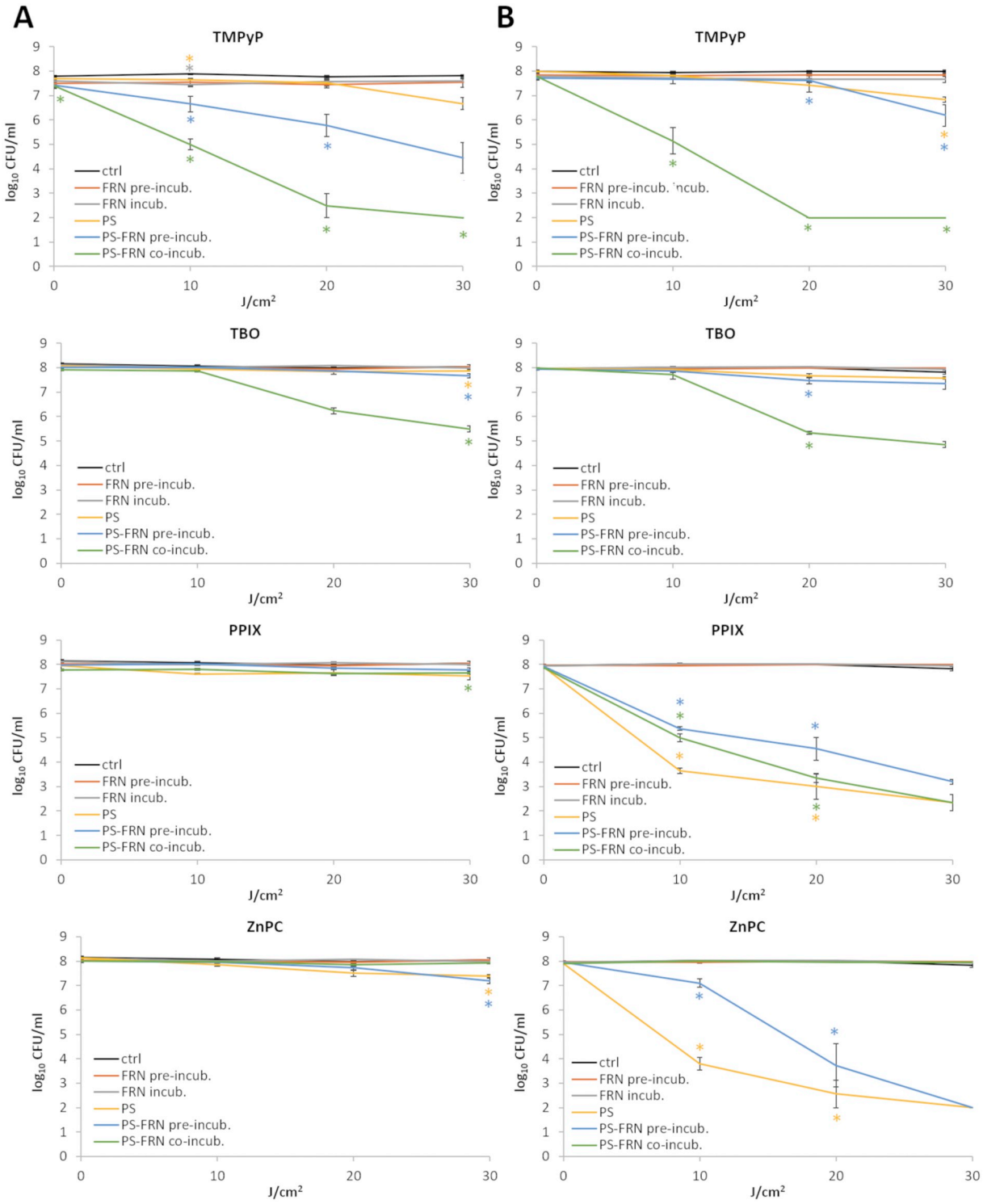

Fig. 1. Phototoxic effect of various PSs and red light against *S. aureus* in the presence of farnesol. Graphs show the *S. aureus* strains SH1000 (A) and RN6390 (B). The concentrations of farnesol used were 70 μM for SH1000, and 35 μM for RN6390. . Viability counts are the mean values of three independent biological experiments. Error bars represent the standard error calculated by dividing the standard deviation by the square root of the number of replicates. Asterisks indicate significance at $p < .015$ according to Student's *t*-test, compared to light controls (0 μM TMPyP, 0 μM FRN). The studied PSs were used at the following concentrations: TMPyP (5,10,15,20-tetrakis(1-methylpyridinium-4-yl)porphyrin tetratosylate), TBO (phenothiazine toluidine blue O), PPIX (protoporphyrin IX) at 20 μM, ZnPC (zinc phthalocyanine) at 5 nM. Ctrl – cells exposed to light only; FRN pre-incub. – cells cultured with FRN for 24 h; FRN incub. - cells incubated with FRN for 30 min; PS – cells treated with respective PS; PS-FRN pre-incub. - cells cultured with FRN for 24 h, incubated with PS and then irradiated; PS-FRN co-incub. - cells incubated with PS and FRN for 30 min. (For interpretation of the references to colour in this figure legend, the reader is referred to the web version of this article.)

Table 2
Phototoxic effect of 20 μM TMPyP, farnesol and red light on *S. aureus* cells.

Strain	Mean reduction of survival[a] (log_{10} CFU) ± SE					
	J/cm^2	TMPyP	FRN pre-incub.	TMPyP FRN pre-incub.	FRN incub.	TMPyP FRN co-incub.
SH1000	0	0.1 ± 0.06	0.0 ± 0.0	0.08 ± 0.05	0.0 ± 0.0	0.20 ± 0.05
	10	0.14 ± 0.05	−0.09 ± 0.01	0.83 ± 0.31	0.16 ± 0.06	2.6 ± 0.21
	20	0.27 ± 0.16	0.06 ± 0.06	1.72 ± 0.55	0.02 ± 0.03	**5.1 ± 0.45**
	30	1.13 ± 0.28	−0.1 ± 0.1	**3.04 ± 0.84**	0.07 ± 0.04	**5.62 ± 0.06**
RN6390	0	0.01 ± 0.03	0.0 ± 0.0	0.14 ± 0.08	0.0 ± 0.0	−0.01 ± 0.02
	10	0.17 ± 0.07	0.02 ± 0.03	0.19 ± 0.12	0.06 ± 0.09	2.64 ± 0.46
	20	0.57 ± 0.32	0.0 ± 0.04	0.22 ± 0.01	0.11 ± 0.04	**5.78 ± 0.11**
	30	1.17 ± 0.15	0.01 ± 0.02	1.67 ± 0.46	0.26 ± 0.19	**5.89 ± 0.05**

The values were calculated by subtracting log_{10} CFU/ml of treated samples from those of untreated controls (0 J/cm^2; 0 μM TMPyP, 0 μM FRN). Bold values indicate a bactericidal effect (> 3 log_{10} reduction units). Underlined values indicate significance at $p < .01$ according to Student's t-test, compared to light controls (0 μM TMPyP, 0 μM farnesol). Results are presented as mean values of three experiments with a standard error calculated by dividing standard deviation per square root of the number of replicates. FRN pre-incub. – bacteria cultured with FRN for 24 h; FRN incub. – bacteria incubated with FRN shortly prior to irradiation; FRN co-incub. – bacteria irradiated with TMPyP and FRN after short incubation with both compounds.
FRN – farnesol; TMPyP - 5,10,15,20-tetrakis(1-methylpyridinium-4-yl)porphyrin tetratosylate.

does not facilitate the penetration of a PS through bacterial envelopes and that some other mechanisms are involved.

3.5. Effect of Farnesol on Bacterial Membrane: Staphyloxanthin Content and Membrane Fluidity

S. aureus sensitivity to PDI, aside from photodynamic properties and the accumulation of a compound, can depend on various bacterial phenotypic features, such as staphyloxanthin content and the degree of bacterial membrane fluidity. Farnesol is a known inhibitor of the staphyloxanthin synthesis pathway in *S. aureus* [37]. This inhibition was confirmed in strain SH1000 after 24 h of growth in the presence of FRN, which lowered the level of carotenoids to the levels observed in the nonpigmented strain RN6390 (Fig. 5). However, taking into account that the best bactericidal effect was achieved after a relatively short treatment, in which bacterial bleaching could not yet be observed, the inhibition of staphyloxanthin synthesis does not seem to be crucial for this phenomenon. A combined bactericidal effect was observed in both strains SH1000 and RN6390 independent of their overall carotenoid content.

Farnesol can alter the structure of the bacterial membrane, which can be detected by means of its fluidity. DPH, a lipophilic fluorescent probe used to observe membrane fluidity, preferentially localizes to hydrophobic (intrinsic) regions of cell membrane phospholipids and emits polarized light upon excitation. The value of fluorescence anisotropy (r) reflects the degree of a fluorophore's free movement that is dependent on membrane fluidity. An inverse relationship occurs between the measured DPH fluorescence anisotropy and membrane fluidity [38]. Temperature-dependent analysis of strain SH1000 revealed a change in membrane structure after FRN treatment. After 30 min of incubation, an increase in membrane fluidity was observed at each measurement point. After 24 h of treatment with FRN, the fluidity was further increased, which is probably connected to the lack of staphyloxanthin in the bacterial membrane (Fig. 6). The analysis of RN6390 also revealed noticeable changes after FRN treatment; however, the initial increase in membrane fluidity subsided after 24 h. The fact that the r values of "bleached" SH1000 did not match those of nonpigmented RN6390 suggests that other factors exist that regulate overall membrane fluidity. Nevertheless, increased fluidity after short FRN treatment suggests a higher degree of structural disorder and can to some extent contribute to the bactericidal effect observed in both strains.

4. Discussion

The present research is the first report describing the use of FRN as an adjuvant in antibacterial PDI. The effect of FRN on PDI efficacy is not common to various types of red light-absorbing PSs. The compounds used in our study included a phenothiazine representative, TBO, and three PSs based on a cyclic tetrapyrrole structure: cationic meso-substituted porphyrin TMPyP, PPIX and zinc phthalocyanine. A strong potentiation of bactericidal action in the presence of FRN was observed only for TMPyP and for a much lesser extent for TBO (Fig. 1). A specific action of FRN and TMPyP occurred shortly after simultaneous incubation and only in the presence of light. With respect to the fact that PDI, as well as farnesol, acts in bacterial cells in a multidirectional manner, a precise mechanism of this specific action is still not fully understood. To explain this unique potentiation of TMPyP-based PDI, we applied a classical approach to analyze the photodynamic properties of TMPyP in combination with FRN. Surprisingly, none of the basic characteristics, including spectral properties, reactive oxygen species formation and PS uptake, provided an explanation for the observed phenomenon. Together with a very diverse effect obtained for other PSs (including abolishing ZnPC bactericidal action), we hypothesize that farnesol affects specific molecular targets crucial for *S. aureus* sensitivity to TMPyP-based PDI. Bacterial membrane proteins and lipids are considered the main molecules affected by PDI [36,39] and specific phospholipids have been reported to be modified in *Staphylococcus warneri* in the presence of cationic porphyrin derivative [40]. Specifically, in the case of TMPyP particular targets have been previously identified in the photoinactivation of nonenveloped RNA viruses [41]. A unique potentiation of this compound further suggests that despite the generally accepted universality of the PDI method, PSs can act through specific molecular mechanisms.

Even though the molecular background of the combined FRN and TMPyP photodynamic action remains unclear, such an outcome is very promising in the context of possible *in vivo* applications due to the possible use of red light. Cationic meso-substituted porphyrin derivatives, such as TMPyP, are generally referred to as potent singlet oxygen producers [23]. The cationic character of these compounds promotes binding to negatively charged bacterial cell surfaces. However, the characteristic structure of these derivatives implies their decreased ability to absorb in a range of red light (molar absorption coefficient determined for Q bands is relatively low compared to unsubstituted porphyrins) [2]. Accordingly, in this phenomenon, meso-substituted porphyrins are often activated with blue or broad-spectrum white light [40,42,43]. As we showed, TMPyP alone irradiated with an applied

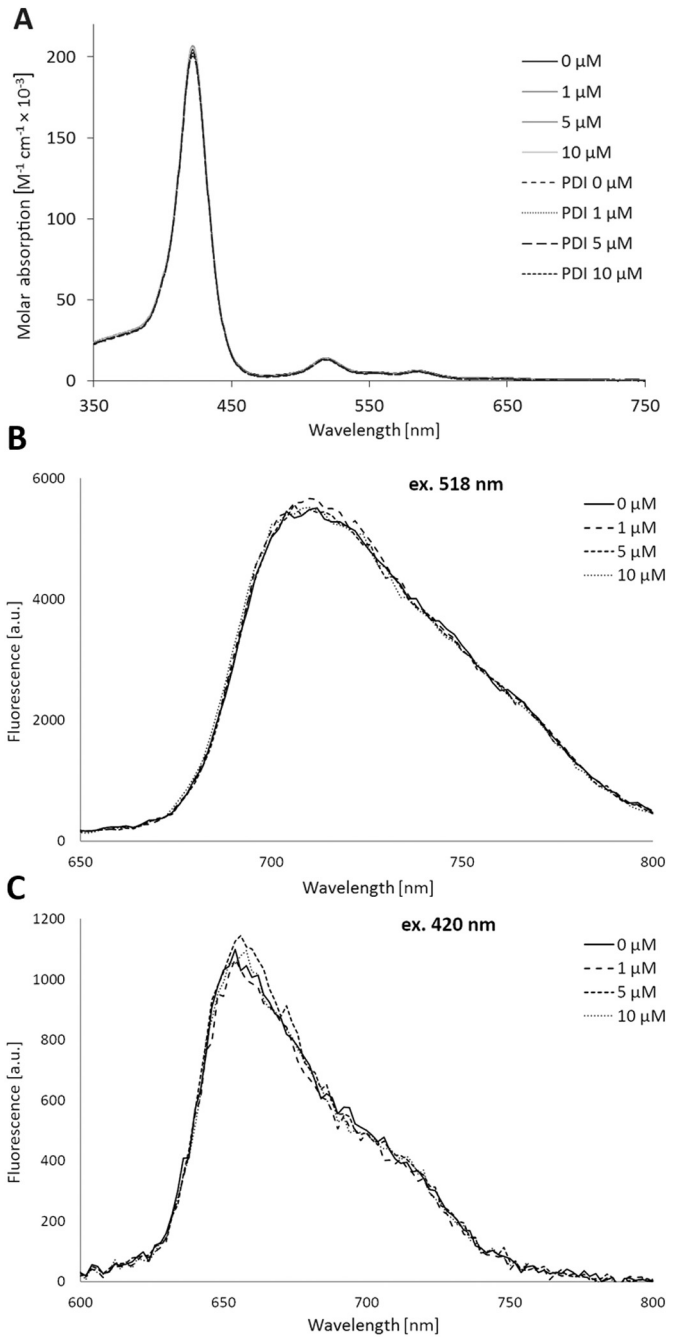

Fig. 2. Molar absorption and fluorescence spectra of 5 µM TMPyP titrated with farnesol. A) Molar absorption spectra of 5 µM TMPyP in water. Solid lines indicate samples titrated with increasing concentrations of FRN and incubated for 30 min at 37 °C in the dark. Dashed lines indicate corresponding samples irradiated with red light at a dose of 20 J/cm^2 (PDI). B) Fluorescence spectra. Graphs show fluorescence emission spectra of 5 µM TMPyP in water exited in Q-band (ex. 518 nm) after titration with increasing concentrations of FRN and incubation for 30 min at 37 °C in the dark. C) Fluorescence emission spectra of 0.05 µM TMPyP in water excited in Soret region (ex. 420 nm) after titration with increasing concentrations of FRN and incubation for 30 min at 37 °C in the dark. A.U. – arbitrary units. Lines present mean values for three independent measurements. (For interpretation of the references to colour in this figure legend, the reader is referred to the web version of this article.)

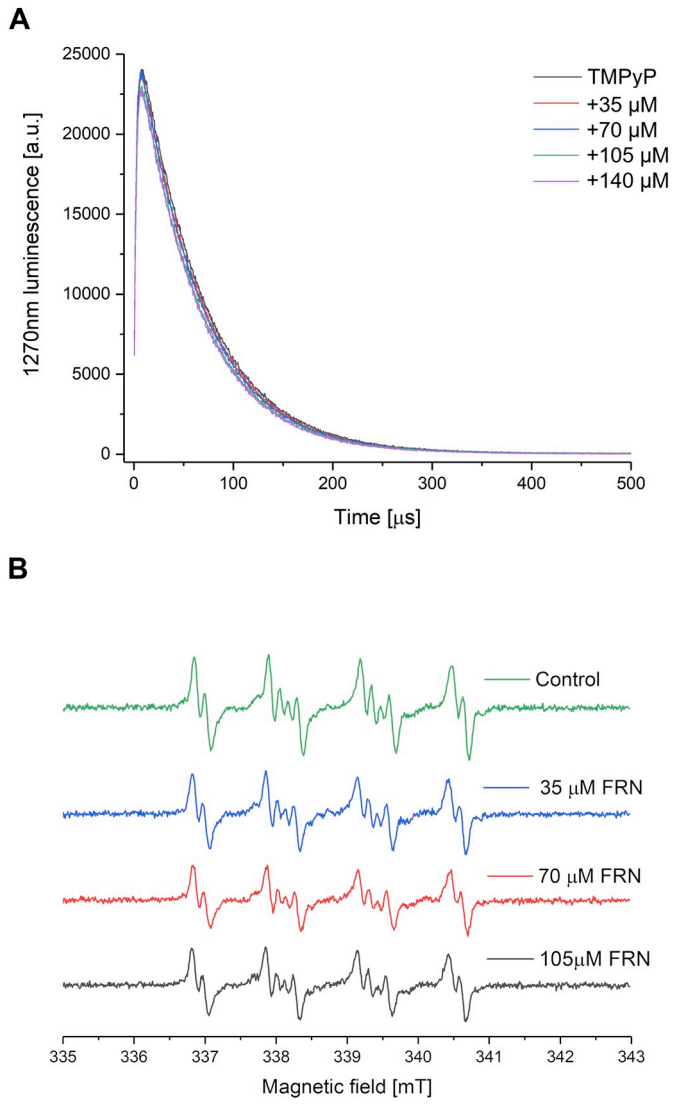

Fig. 3. Reactive oxygen species formation in the presence of farnesol. A) Time-resolved detection of singlet oxygen phosphorescence. Signals were recorded for 20 µM TMPyP alone and with the addition of increasing concentrations of farnesol. B) Detection of superoxide anions generated by TMPyP at a 20 µM concentration. The pattern of superoxide spin amplitude was compared with the signal generated after the addition of 35 µM farnesol.

light source (λ_{max} 632 nm) remained ineffective at the photodynamic killing of *S. aureus*; however, in combination with farnesol and red light, a pronounced bactericidal effect can be achieved. The observed phenomenon enables the use of wavelengths that are beneficial for therapeutic use. Shorter wavelengths can be strongly absorbed by blood and scattered by biological structures. The more redshifted the visible light used in PDI is, the more efficient is the tissue penetration [44].

The unclear mechanism of the TMPyP and FRN combined action is connected to the complex nature of PDI and to the elusive pleiotropic effect caused by FRN in bacterial cells. The antibacterial activity of farnesol, as well as its role in the potentiation of antibacterial agents, has been described in the literature, especially for gram-positive bacteria [21,22,45,46]. Its primary mode of action has been attributed to the disruption of the cell membrane that occurs shortly after exposure, causing a drastic release of K^+ ions without affecting potassium channels [47,48]. The affinity of FRN for bacterial membranes results from its hydrophobic nature. It has also been reported that the morphology of *S. aureus* cells treated with a high concentration of FRN was similar to that caused by cell wall-active antibiotics [49]. With respect to this mode of action, FRN in combination with antibacterials is believed to facilitate the penetration of compounds and to enhance their bactericidal action at lower concentrations [20–22]. Apart from altering the structure of the bacterial cell envelope, FRN seems to induce multiple

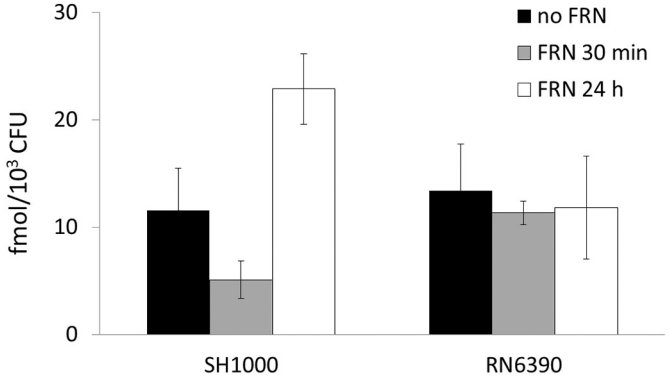

Fig. 4. Accumulation of TMPyP in *S. aureus*. Bacterial cells were incubated with 20 μM TMPyP. The concentration of TMPyP remaining in PBS after incubation was calculated, resulting in the fmol of a PS accumulated per 1000 cells. Boxes represent the mean values of three biological replicates for samples without FRN, with FRN at subinhibitory concentration (70 μM for SH1000 and 35 μM for RN6390) added 30 min before measurement and samples preincubated with FRN for 24 h. Error bars represent the standard error calculated by dividing standard deviation by the square root of the number of replicates.

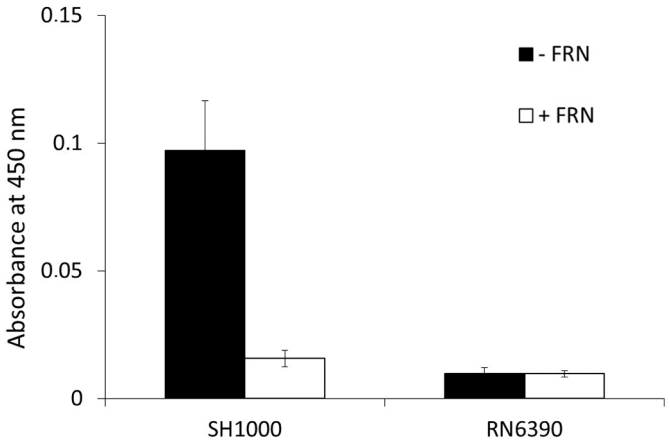

Fig. 5. Carotenoid content after treatment with farnesol. Bacteria were grown at subinhibitory concentrations of FRN (70 μM for SH1000 and 35 μM for RN6390) for 24 h, and the absorbance of methanol extracts was measured. Boxes represent the mean values of three biological replicates. Error bars represent the standard error calculated by dividing the standard deviation by the square root of the number of replicates.

metabolic changes in *S. aureus*, some of which have been described in the literature. FRN blocks an initial stage in the staphyloxanthin synthesis pathway, where, due to its structural analogy to farnesyl pyrophosphate, it binds the dehydrosqualen synthase CrtM and prevents all further carotenoid compound formation [37]. FRN also competitively inhibits the activity of a staphylococcal lipase [50] and affects fibrin fiber formation by inhibiting coagulase [49]. Another process affected by FRN in *S. aureus* is the recycling of the C_{55} lipid carrier of the murein monomer precursor, which leads to the disruption of cell wall biosynthesis [37]. Moreover, FRN affects the mevalonate pathway by inhibiting staphylococcal HMG-CoA reductase, which leads to growth inhibition [51]. It is also an agent known to prevent biofilm formation in *S. aureus* and coagulase-negative staphylococci [20,46,52]. In another microorganism, *C. albicans*, farnesol acts as a quorum-sensing molecule, where it prevents the transition from yeast to hyphal growth and compromises biofilm formation [19]. In *S. aureus,* however, it is doubtful that the antimicrobial effect of FRN depends on this quorum-sensing mechanism, as this crosstalk in staphylococci involves mainly autoinducing peptides and the accessory gene regulator system [20].

As shown in this report, FRN also enhanced the PDI of *S. aureus*. Several attempts have been undertaken to explain the observed potentiation of red light-activated TMPyP by this multifunctional sesquiterpenoid. First, we investigated the possibility that farnesol interacts with TMPyP and forms a toxic intermediate or improves the action of the PS by modulating the absorption capability. However, the antibacterial activity of farnesol was not increased by TMPyP as evidenced by MIC values and dark toxicity in PDI experiments (Tables 1 and 2). Additionally, no changes in TMPyP absorption and fluorescence spectra in the presence of FRN were observed, even in irradiated samples (Fig. 2). Since oxidative stress is an inherent element of PDI, we also analyzed reactive oxygen species generation in the presence of FRN. The potential formation of ROS in *S. aureus* upon FRN treatment has been analyzed and described in the literature. Inoue et al. reported that farnesol does not induce the formation of ROS in planktonic *S. aureus* culture [48]. On the other hand, in the case of *S. aureus* biofilm, the FRN produced by *C. albicans* promoted intracellular ROS accumulation, as described elsewhere [53]. It was also shown that FRN inhibited oxidation-reduction reactions in *S. aureus* [20] and *S. epidermidis* [46]. However, the experiments conducted in the present work revealed no influence of FRN on the ROS generation induced by TMPyP (Fig. 3). This confirms that the mechanism of the observed phenomenon does not depend on the modulation of TMPyP photodynamic properties. We should also take into consideration that ROS generated by excited TMPyP during PDI can affect farnesol molecules resulting in formation of a toxic product. However, since all analyzed photosensitizers are generally referred to as potent singlet oxygen producers, the expected bactericidal effect in a presence of farnesol would be observed for all used compounds. The observed phenomenon also cannot be explained by the amount of PS accumulated by *S. aureus* under the analyzed conditions (Fig. 4). Incubation with farnesol did not enhance TMPyP uptake, which suggests no increased penetration of the PS in the dark. It is worth mentioning, however, that the applied method quantitatively measured PS uptake, but it did not determine the location of the compound inside a bacterial cell. In general, TMPyP accumulation in the cytosol or cell wall of *S. aureus* is considered minor during incubation in the dark, and TMPyP only enters following cell wall damage [54]. Once in the cell, TMPyP has the potential to bind DNA [55]; however, high intracellular concentrations of this PS are needed to evoke DNA damage in bacteria [56].

It is worth noting that the reported effect is independent of the genetic background involving *rsbU* gene status, which affects the synthesis capability of staphyloxanthin. Under basic PDI conditions (without FRN), the strains SH1000 and RN6390 responded differently to other tetrapyrrole-based PSs, namely, PPIX and ZnPC (Fig. 1). The PDI experiments revealed that the bactericidal effect of combined TMPyP, farnesol and red light towards both strains was equal and occurred shortly after FRN addition (Table 2). Bacterial killing was much more prominent under these conditions than under conditions in which PDI was applied to cells preincubated (cultured for 24 h) with FRN. This outcome somehow negates the contribution of the metabolism alteration induced by FRN in *S. aureus* and suggests a more rapid reaction. During growth in the presence of FRN, the staphyloxanthin synthesis pathway is inhibited at a preliminary stage, resulting in the lack of the whole pool of carotenoids (Fig. 5). Although carotenoid content was previously described as a significant factor of PDI outcome in *S. aureus* [26], it does not significantly affect response to red light-activated TMPyP. In another aspect, FRN induces the reorganization of membrane structure, which is reflected by the increase in its fluidity. This process is indirectly connected to the lack of staphyloxanthin, which plays a role in maintaining bacterial membrane rigidity similar to that of cholesterol in mammalian cells [57]. An increase in membrane fluidity upon incubation with FRN was observed in both strains SH1000 and RN6390 (Fig. 6). In the former strain, the effect was dependent on the incubation time with farnesol. For strain RN6390, this trend was not clear; however, in the presence of FRN, membrane fluidity was

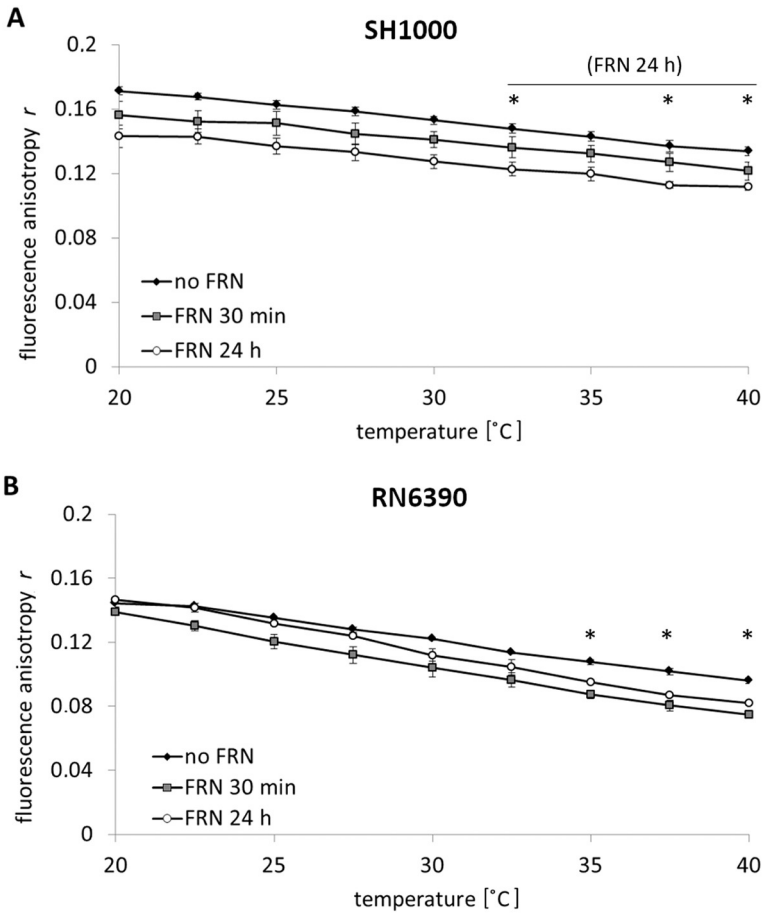

Fig. 6. Fluorescence anisotropy of the DPH that accumulated in the bacterial membrane in a temperature gradient. A) strain SH1000, B) strain RN6390. An inverse relationship between the measured DPH fluorescence anisotropy and membrane fluidity occurs was observed. Plots show the mean values of two to three biological replicates of samples without FRN, with FRN at subinhibitory concentrations (70 μM for SH1000 and 35 μM for RN6390) added 30 min before protoplast formation and samples preincubated (cultured) with FRN for 24 h. Error bars represent the standard error calculated by dividing the standard deviation by the square root of the number of replicates. Significance at $p < .05$ according to Student's *t*-test is marked with asterisks. For strain SH1000, this level of significance was achieved only after a 24 h preincubation with FRN at the indicated measurement points (white circles). For strain RN6390, significance was achieved after 30 min of incubation and after preincubation with FRN.

increased. This outcome is probably connected to a natural lack of staphyloxanthin in this strain and suggests that changes in membrane structure occur shortly after FRN addition regardless of staphyloxanthin level. As reported by Inoue et al., an increase in membrane fluidity was observed mainly in the superficial layer only after 3 min of exposure to high FRN concentrations [48]. It is worth mentioning, however, that the concentrations of FRN used in our study were lower than in the concentrations used in most previous reports.

Our results suggest that the potentiation of red light-activated TMPyP is specific, rapid and does not influence PS photodynamic properties by means of spectral changes and ROS generation. The identification of the mechanisms and molecular targets involved in the observed phenomenon requires further investigation. The combined action of farnesol and TMPyP opens a new path in searching for adjuvants in antibacterial PDI.

Acknowledgements and Funding

We thank Dr. Szymon Ziętkiewicz for help in performing membrane fluidity measurements and Dr. Grzegorz Gołuński and Agnieszka Borowik for help in absorption measurement. This wo rk was supported by the grant of National Science Centre (Poland) PRELUDIUM no. 2015/19/N/NZ7/01012.

Declaration of Competing Interest

The authors declare that they have no known competing financial interests or personal relationships that could have appeared to influence the work reported in this paper.

References

[1] A. Shittu, E. Udo, J. Lin, Insights on virulence and antibiotic resistance: a review of the accessory genome of *Staphylococcus aureus*, Wounds. 19 (2007) 237–244.
[2] M. Wainwright, Photodynamic antimicrobial chemotherapy (PACT), J. Antimicrob. Chemother. 42 (1998) 13–28, https://doi.org/10.1093/jac/42.1.13.
[3] M. Bhatti, A. MacRobert, B. Henderson, P. Shepherd, J. Cridland, M. Wilson, Antibody-targeted lethal photosensitization of *Porphyromonas gingivalis*, Antimicrob. Agents Chemother. 44 (2000) 2615–2618, https://doi.org/10.1128/AAC.44.10.2615-2618.2000.
[4] M.L. Embleton, S.P. Nair, B.D. Cookson, M. Wilson, Antibody-directed photodynamic therapy of methicillin resistant *Staphylococcus aureus*, Microb. Drug Resist. 10 (2004) 92–97, https://doi.org/10.1089/1076629041310000.
[5] R. Dosselli, M. Gobbo, E. Bolognini, S. Campestrini, E. Reddi, Porphyrin-apidaecin conjugate as a new broad spectrum antibacterial agent, ACS Med. Chem. Lett. 1 (2010) 35–38, https://doi.org/10.1021/ml900021y.
[6] R. Dosselli, R. Ruiz-González, F. Moret, V. Agnolon, C. Compagnin, M. Mognato, V. Sella, M. Agut, S. Nonell, M. Gobbo, E. Reddi, Synthesis, spectroscopic, and photophysical characterization and photosensitizing activity toward prokaryotic and eukaryotic cells of porphyrin-magainin and -buforin conjugates, J. Med. Chem. 57 (2014) 1403–1415, https://doi.org/10.1021/jm401653r.
[7] M.L. Embleton, S.P. Nair, W. Heywood, D.C. Menon, B.D. Cookson, M. Wilson, Development of a novel targeting system for lethal photosensitization of antibiotic-resistant strains of *Staphylococcus aureus*, Antimicrob. Agents Chemother. 49 (2005) 3690–3696, https://doi.org/10.1128/AAC.49.9.3690-3696.2005.
[8] B. Rout, C.H. Liu, W.C. Wu, Photosensitizer in lipid nanoparticle: a nano-scaled approach to antibacterial function, Sci. Rep. 7 (2017) 1–14, https://doi.org/10.1038/s41598-017-07444-w.
[9] T. Tsai, H.F. Chien, T.H. Wang, C.T. Huang, Y.B. Ker, C.T. Chen, Chitosan augments photodynamic inactivation of gram-positive and gram-negative bacteria, Antimicrob. Agents Chemother. 55 (2011) 1883–1890, https://doi.org/10.1128/AAC.00550-10.
[10] J. Nakonieczna, A. Rapacka-Zdonczyk, A. Kawiak, K.P. Bielawski, M. Grinholc, Sublethal photodynamic inactivation renders *Staphylococcus aureus* susceptible to silver nanoparticles, Photochem. Photobiol. Sci. (2013), https://doi.org/10.1039/c3pp50039j.
[11] J. Nakonieczna, K. Wolnikowska, P. Ogonowska, D. Neubauer, A. Bernat, W. Kamysz, Rose bengal-mediated photoinactivation of multidrug resistant *Pseudomonas aeruginosa* is enhanced in the presence of antimicrobial peptides, Front. Microbiol. 9 (2018) 1–15, https://doi.org/10.3389/fmicb.2018.01949.

[12] A. Wozniak, M. Grinholc, Combined antimicrobial activity of photodynamic inactivation and antimicrobials-state of the art, Front. Microbiol. 9 (2018), https://doi.org/10.3389/fmicb.2018.00930.

[13] A. Wozniak, A. Rapacka-Zdonczyk, N.T. Mutters, M. Grinholc, Antimicrobials are a photodynamic inactivation adjuvant for the eradication of extensively drug-resistant *Acinetobacter baumannii*, Front. Microbiol. (2019), https://doi.org/10.3389/fmicb.2019.00229.

[14] M.Q. Mesquita, C.J. Dias, M.G.P.M.S. Neves, A. Almeida, M.A.F. Faustino, Revisiting current photoactive materials for antimicrobial photodynamic therapy, Molecules 23 (2018), https://doi.org/10.3390/molecules23102424.

[15] A.G. Staines, P. Sindelar, M.W.H. Coughtrie, B. Burchell, Farnesol is glucuronidated in human liver, kidney and intestine *in vitro*, and is a novel substrate for UGT2B7 and UGT1A1, Biochem. J. 384 (2004) 637–645, https://doi.org/10.1042/BJ20040997.

[16] R.E. Duncan, M.C. Archer, Farnesol induces thyroid hormone receptor (THR) β1 but inhibits THR-mediated signaling in MCF-7 human breast cancer cells, Biochem. Biophys. Res. Commun. (2006), https://doi.org/10.1016/j.bbrc.2006.02.145.

[17] E.M. Yazlovitskaya, G. Melnykovych, Selective farnesol toxicity and translocation of protein kinase C in neoplastic HeLa-S3K and non-neoplastic CF-3 cells, Cancer Lett. (1995), https://doi.org/10.1016/0304-3835(94)03635-V.

[18] A. Rioja, A.R. Pizzey, C.M. Marson, N.S.B. Thomas, Preferential induction of apoptosis of leukaemic cells by farnesol, FEBS Lett. 467 (2000) 291–295, https://doi.org/10.1016/S0014-5793(00)01168-6.

[19] G. Ramage, S.P. Saville, B.L. Wickes, J.L. López-Ribot, Inhibition of *Candida albicans*biofilm formation by farnesol, a quorum-sensing molecule, Appl. Environ. Microbiol. (2002), https://doi.org/10.1128/AEM.68.11.5459-5463.2002.

[20] M.A. Jabra-Rizk, T.F. Meiller, C.E. James, M.E. Shirtliff, Effect of farnesol on *Staphylococcus aureus* biofilm formation and antimicrobial susceptibility, Antimicrob. Agents Chemother. (2006), https://doi.org/10.1128/AAC.50.4.1463-1469.2006.

[21] B.F. Brehm-Stecher, E.A. Johnson, Sensitization of *Staphylococcus aureus* and *Escherichia coli* to antibiotics by the sesquiterpenoids nerolidol, farnesol, bisabolol, and apritone, Antimicrob. Agents Chemother. (2003), https://doi.org/10.1128/AAC.47.10.3357-3360.2003.

[22] F. Gomes, B. Leite, P. Teixeira, N. Cerca, J. Azeredo, R. Oliveira, Farnesol as antibiotics adjuvant in *Staphylococcus epidermidis* control *in vitro*, Am J Med Sci (2011), https://doi.org/10.1097/MAJ.0b013e3181fcf138.

[23] N.G. Angeli, M.G. Lagorio, E.A.S. Román, L.E. Dicelio, Meso-substituted cationic porphyrins of biological interest. Photophysical and physicochemical properties in solution and bound to liposomes, Photochem. Photobiol. (2004), https://doi.org/10.1562/0031-8655(2000)072<0049:mscpob>2.0.co;2.

[24] C. Pérez-Arnaiz, N. Busto, J. Santolaya, J.M. Leal, G. Barone, B. García, Kinetic evidence for interaction of TMPyP4 with two different G-quadruplex conformations of human telomeric DNA, Biochim. Biophys. Acta, Gen. Subj. 1862 (2018) 522–531, https://doi.org/10.1016/j.bbagen.2017.10.020.

[25] M.J. Cheng, Y.G. Cao, TMPYP4 exerted antitumor effects in human cervical cancer cells through activation of p38 mitogen-activated protein kinase, Biol. Res. 50 (2017) 1–7, https://doi.org/10.1186/s40659-017-0129-4.

[26] M. Kossakowska-Zwierucho, R. Kaźmierkiewicz, K.P. Bielawski, J. Nakonieczna, Factors determining *Staphylococcus aureus*susceptibility to photoantimicrobial chemotherapy: RsbU activity, staphyloxanthin level, and membrane fluidity, Front. Microbiol. 7 (2016) 1–14, https://doi.org/10.3389/fmicb.2016.01141.

[27] M. Wright Valderas, J.W. Gatson, N. Wreyford, M.E. Hart, The superoxide dismutase gene sodM is unique to *Staphylococcus aureus*: absence of sodM in coagulase-negative staphylococci, J. Bacteriol. 184 (2002) 2465–2472, https://doi.org/10.1128/JB.184.9.2465-2472.2002.

[28] M.J. Horsburgh, J.L. Aish, I.J. White, L. Shaw, J.K. Lithgow, S.J. Foster, SigmaB modulates virulence determinant expression and stress resistance: characterization of a functional rsbU strain derived from *Staphylococcus aureus* 8325-4, J. Bacteriol. 184 (2002) 5457–5467, https://doi.org/10.1128/JB.184.19.5457-5467.2002.

[29] A.S. Bayer, R. Prasad, J. Chandra, A. Koul, M. Smriti, A. Varma, R.A. Skurray, N. Firth, M.H. Brown, S.U.P. Koo, M.R. Yeaman, *In vitro* resistance of *Staphylococcus aureus* to thrombin-induced platelet microbicidal protein is associated with alterations in cytoplasmic membrane fluidity, Infect. Immun. 68 (2000) 3548–3553, https://doi.org/10.1128/IAI.68.6.3548-3553.2000.

[30] P. Ogonowska, A. Woźniak, M.K. Pierański, T. Wasylew, P. Kwiek, M. Brasel, M. Grinholc, J. Nakonieczna, Application and characterization of light-emitting diodes for photodynamic inactivation of bacteria, Light. Res. Technol. 51 (2019) 612–624, https://doi.org/10.1177/1477153518781478.

[31] M. Zhang, H.V. Powell, S.R. Mackenzie, P.R. Unwin, Kinetics of porphyrin adsorption and DNA-assisted desorption at the silica-water interface, Langmuir (2010), https://doi.org/10.1021/la903438p.

[32] G. Szewczyk, A. Zadlo, M. Sarna, S. Ito, K. Wakamatsu, T. Sarna, Aerobic photoreactivity of synthetic eumelanins and pheomelanins: generation of singlet oxygen and superoxide anion, Pigment Cell Melanoma Res. 29 (2016) 669–678, https://doi.org/10.1111/pcmr.12514.

[33] A. Lipovsky, Y. Nitzan, H. Friedmann, R. Lubart, Sensitivity of *Staphylococcus aureus*strains to broadband visible light, Photochem. Photobiol. 85 (2009) 255–260, https://doi.org/10.1111/j.1751-1097.2008.00429.x.

[34] D. Voss, T.J. Montville, 1,6-Diphenyl-1,3,5-hexatrine as a reporter of inner spore membrane fluidity in *Bacillus subtilis* and *Alicyclobacillus acidoterrestris*, J. Microbiol. Methods 96 (2014) 101–103, https://doi.org/10.1016/j.mimet.2013.11.009.

[35] K.T. Bæk, D. Frees, A. Renzoni, C. Barras, N. Rodriguez, W.L. Kelley, Genetic variation in the *Staphylococcus aureus* 8325 strain lineage revealed by whole-genome sequencing, PLoS One 8 (2013) 1–16, https://doi.org/10.1371/journal.pone.0077122.

[36] E. Alves, M.A. Faustino, M.G. Neves, A. Cunha, J. Tome, A. Almeida, An insight on bacterial cellular targets of photodynamic inactivation, Future Med. Chem. 6 (2014) 141–164, https://doi.org/10.4155/fmc.13.211.

[37] M. Kuroda, S. Nagasaki, T. Ohta, Sesquiterpene farnesol inhibits recycling of the C55 lipid carrier of the murein monomer precursor contributing to increased susceptibility to β-lactams in methicillin-resistant *Staphylococcus aureus*, J. Antimicrob. Chemother. 59 (2007) 425–432, https://doi.org/10.1093/jac/dkl519.

[38] N.N. Mishra, G.Y. Liu, M.R. Yeaman, C.C. Nast, R.A. Proctor, J. McKinnell, A.S. Bayer, Carotenoid-related alteration of cell membrane fluidity impacts *Staphylococcus aureus* susceptibility to host defense peptides, Antimicrob. Agents Chemother. 55 (2011) 526–531, https://doi.org/10.1128/AAC.00680-10.

[39] E. Alves, C. Moreirinha, M.A.F. Faustino, Â. Cunha, I. Delgadillo, M.G.P.M.S. Neves, A. Almeida, Overall biochemical changes in bacteria photosensitized with cationic porphyrins monitored by infrared spectroscopy, Future Med. Chem. 8 (2016) 613–628, https://doi.org/10.4155/fmc-2015-0008.

[40] E. Alves, T. Melo, C. Simões, M.A.F. Faustino, J.P.C. Tomé, M.G.P.M.S. Neves, J.A.S. Cavaleiro, Â. Cunha, N.C.M. Gomes, P. Domingues, M.R.M. Domingues, A. Almeida, Photodynamic oxidation of *Staphylococcus warneri* membrane phospholipids: new insights based on lipidomics, Rapid Commun. Mass Spectrom. 27 (2013) 1607–1618, https://doi.org/10.1002/rcm.6614.

[41] H. Majiya, O.O. Adeyemi, M. Herod, N.J. Stonehouse, P. Millner, Photodynamic inactivation of non-enveloped RNA viruses, J. Photochem. Photobiol. B Biol. 189 (2018) 87–94, https://doi.org/10.1016/j.jphotobiol.2018.10.009.

[42] R. Dosselli, R. Millioni, L. Puricelli, P. Tessari, G. Arrigoni, C. Franchin, A. Segalla, E. Teardo, E. Reddi, Molecular targets of antimicrobial photodynamic therapy identified by a proteomic approach, J. Proteome 77 (2012) 329–343, https://doi.org/10.1016/j.jprot.2012.09.007.

[43] A. Hanakova, K. Bogdanova, K. Tomankova, K. Pizova, J. Malohlava, S. Binder, R. Bajgar, K. Langova, M. Kolar, J. Mosinger, H. Kolarova, The application of antimicrobial photodynamic therapy on *S. aureus* and *E. coli* using porphyrin photosensitizers bound to cyclodextrin, Microbiol. Res. 169 (2014) 163–170, https://doi.org/10.1016/j.micres.2013.07.005.

[44] Z. Sun, L.P. Zhang, F. Wu, Y. Zhao, Photosensitizers for two-photon excited photodynamic therapy, Adv. Funct. Mater. (2017), https://doi.org/10.1002/adfm.201704079.

[45] H. Koo, M.F. Hayacibara, B.D. Schobel, J.A. Cury, P.L. Rosalen, Y.K. Park, A.M. Vacca-Smith, W.H. Bowen, Inhibition of *Streptococcus mutans* biofilm accumulation and polysaccharide production by apigenin and tt-farnesol, J. Antimicrob. Chemother. 52 (2003) 782–789, https://doi.org/10.1093/jac/dkg449.

[46] F.I.A. Gomes, P. Teixeira, J. Azeredo, R. Oliveira, Effect of farnesol on planktonic and biofilm cells of *Staphylococcus epidermidis*, Curr. Microbiol. (2009), https://doi.org/10.1007/s00284-009-9408-9.

[47] Y. Inoue, A. Shiraishi, T. Hada, K. Hirose, H. Hamashima, J. Shimada, The antibacterial effects of terpene alcohols on *Staphylococcus aureus* and their mode of action, FEMS Microbiol. Lett. (2004), https://doi.org/10.1016/j.femsle.2004.06.049.

[48] Y. Inoue, N. Togashi, H. Hamashima, Farnesol-induced disruption of the *Staphylococcus aureus* cytoplasmic membrane, Biol. Pharm. Bull. Pharm. Bull. (2016), https://doi.org/10.1248/bpb.b15-00416.

[49] H. Akiyama, T. Oono, W.K. Huh, O. Yamasaki, S. Ogawa, M. Katsuyama, H. Ichikawa, K. Iwatsuki, Actions of farnesol and xylitol against *Staphylococcus aureus*, Chemotherapy (2002), https://doi.org/10.1159/000064916.

[50] M. Kuroda, S. Nagasaki, R. Ito, T. Ohta, Sesquiterpene farnesol as a competitive inhibitor of lipase activity of *Staphylococcus aureus*, FEMS Microbiol. Lett. 273 (2007) 28–34, https://doi.org/10.1111/j.1574-6968.2007.00772.x.

[51] M. Kaneko, N. Togashi, H. Hamashima, M. Hirohara, Y. Inoue, Effect of farnesol on mevalonate pathway of *Staphylococcus aureus*, J. Antibiot. (Tokyo). (2011). doi:https://doi.org/10.1038/ja.2011.49.

[52] A. Unnanuntana, L. Bonsignore, M.E. Shirtliff, E.M. Greenfield, The effects of farnesol on *Staphylococcus aureus* biofilms and osteoblasts. An *in vitro* study, J. Bone Joint Surg. Am. 91 (2009) 2683–2692, https://doi.org/10.2106/JBJS.H.01699.

[53] E.F. Kong, C. Tsui, S. Kucharíková, P. Van Dijck, M.A. Jabra-Rizk, Modulation of *Staphylococcus aureus* response to antimicrobials by the *Candida albicans*quorum sensing molecule farnesol, Antimicrob. Agents Chemother. (2017), https://doi.org/10.1128/aac.01573-17.

[54] A. Gollmer, A. Felgentraeger, T. Maisch, C. Flors, Real-time imaging of photodynamic action in bacteria, J. Biophotonics 10 (2017) 264–270, https://doi.org/10.1002/jbio.201500259.

[55] N.S. Lebedeva, E.S. Yurina, Y.A. Gubarev, S.A. Syrbu, Interactions of tetracationic porphyrins with DNA and their effects on DNA cleavage, Spectrochim. Acta - A Mol. Biomol. Spectrosc. 199 (2018) 235–241, https://doi.org/10.1016/j.saa.2018.03.066.

[56] F. Cieplik, D. Deng, W. Crielaard, W. Buchalla, E. Hellwig, A. Al-Ahmad, T. Maisch, Antimicrobial photodynamic therapy–what we know and what we don't, Crit. Rev. Microbiol. 44 (2018) 571–589, https://doi.org/10.1080/1040841X.2018.1467876.

[57] C.I. Liu, G.Y. Liu, Y. Song, F. Yin, M.E. Hensler, W.Y. Jeng, V. Nizet, A.H.J. Wang, E. Oldfield, A cholesterol biosynthesis inhibitor blocks *Staphylococcus aureus* virulence, Science (80-.) (2008), https://doi.org/10.1126/science.1153018.